Nano Rotor Blade Airfoil Optimization

Zhen Liu[1]*, Longlei Dong[1]†, Jean-marc Moschetta[2]‡
and Jianping Zhao[1]§

[1] Xi'an Jiaotong University, Xi'an, China
liuz@mail.xjtu.edu.cn,dongll@mail.xjtu.edu.cn,zhaojianping@mail.xjtu.edu.cn
[2] Institut Supérieur de l'Aéronautique et de l'Espace, Toulouse, France
jean-marc.moschetta@isae.fr

Abstract

The aerodynamic performance of airfoil at ultra-low Re has a great impact on the propulsive performance of nano rotor. Therefore, the optimization of airfoil is necessary before the design of nano rotor. Nano rotor blade airfoil optimization is a multi-objective problem since the airfoil suffers a wide range of Reynolds number which increases the difficulty of optimization. In this paper,the airfoil of nano rotor was optimized based on the controlled elitist Non-dominated Sorting Genetic Algorithm II (NSGA-II) coupling with the parameterization method of Class function/Shape function Transformation technique (CST) and the multi-objectives function processing method of statistic definition of stability. An airfoil was achieved with a thickness of 2% and a maximum camber of 5.6% at 2/3 of chord. Optimized airfoil exhibits a good aerodynamic performance at ultra-low Re according to the simulation with CFD solver based on 2D incompressible NS equation. And comparisons were carried out between the performance of the rotors designed with designed airfoil and ag38 airfoil, which showed that the optimized airfoil was suitable for rotor design.

http://www.imavs.org/

Contents

1 Introduction **2**

2 Geometry Parametric Representation and Aerodynamic Solver **4**
2.1 Geometry Parametric Representation 4
2.2 Aerodynamic Solver 5

3 Objective Function Definition Method and Optimization Method **7**
3.1 Objective Function Definition Method 7
3.2 Optimization Method 7

4 Results and Discussion **9**

5 Conclusion **13**

6 Future Work **14**

7 Acknowledgments **14**

*Lecturer, State Key Laboratory for Strength and Vibration of Mechanical Structures, school of Aerospace; corresponding author.

†Associate Professor, State Key Laboratory for Strength and Vibration of Mechanical Structures, school of Aerospace.

‡Professor, Department of Aerodynamics, Energetics and Propulsion.

§Engineer, State Key Laboratory for Strength and Vibration of Mechanical Structures, school of Aerospace.

http://www.imavs.org/

1 Introduction

Rotary-wing Nano Air Vehicle (NAV) is typically a configuration for NAV design. The propulsive performance of rotor determines the flight performance of NAV directly. It is therefore necessary to design the rotor so as to obtain an excellent propulsive performance. As the aerodynamic performance of nano rotor blade airfoil remarkably influences on nano rotor performance, the airfoil optimization is an important part of rotor design. However, the study of nano rotor airfoil is rarely performed. SAMARAI, a rotary-wing NAV, employs directly AG38 thick airfoil [44], and the other design of nano rotor selected the existing low-Re airfoil as well [17]. Therefore, the optimization of nano rotor airfoil requires to be carried out.

Typical airfoil optimization includes the selection of aerodynamic solver, the process of objective function, the geometry parametric representation of airfoil and airfoil optimization method etc. It is a challenge to combine all the parts together to design an excellent airfoil for nano rotor because of its special working condition. Firstly, nano rotor optimization requires an efficient and accurate aerodynamic solver at ultra-low Reynolds number. Nano rotor operates at ultra-low Reynolds number lower than 20000 because of its small dimension resulting in difficulties of optimization. Since the computational resource and time are enormous for an airfoil optimization, an accurate and efficient solver is preferable. Navier-Stokes solver coupling with grid generation method are utilized for optimization of airfoil [34, 41, 38] in recent years but it requires enormous computational cost. Vortex panel method method such as XFoil is also popular for optimization of airfoil due to its time-saving characteristics especially with fairly good results at low Reynolds number. Besides, the optimization of nano rotor blade airfoil is a multi-objective problem to achieve an airfoil with excellent aerodynamic performance along different stations of rotor blade. Because nano rotor are usually both tapered and twisted and the relative velocity of blade section is proportional to the distance from the rotational center along the blade, nano airfoil blade rotor suffers a wide Reynolds number ranging from 6000 to 16000 taking into account the hub. So the optimized airfoil shall process excellent aerodynamic performance at different Reynolds numbers. Kunz [24] utilized the lift-to-drag as the objective to optimize the airfoil separately at two Reynolds numbers. For the single-point optimization, the aerodynamic performance of airfoil may degrade at off-design point. Most optimizations take the value of objectives at design points as objective functions resulting in the irregular airfoil form especially for multi-objective optimizations. Some studies utilized multi-point optimization method to take into account several Res [11]. However, the optimal airfoil was always achieved with corrugated surface. Li and Padula [26] proposed statistical definition of stability method in which the mean value and the standard deviation of values of objectives at design points are taken as the final objective functions. This method ensures the optimized results at each design points and the smoothness of airfoil form.

Airfoil optimization method is also a key point for nano rotor blade airfoil optimization. In the past decades, many methods, which are basically divided into two categories: inverse method and direct method, have been proposed to get the form of airfoil directly with the flight condition. Selig et al. [36, 35] developed a multi-point inverse method to design airfoil with conformal mapping. With the development of computational techniques and algorithm method, the direct methods which allow the process of more complicate problem were applied on the optimization of airfoil. Kunz and Kroo [21] performed computation study of airfoil for rotary wing at Re from 2,000 to 6,000 and the optimizations of NACA airfoil based on gradient method. Nemec [28] and Burgree [6] utilized gradient-based numerical optimizations methods to fulfill the aerodynamic design problem. Alexandron et al. [2] applied the Approximation and Model Management Framework (AMMF), which has the capacity of rapid and early integration of

http://www.imavs.org/

high fidelity nonlinear analyses and experimental results into the multidisciplinary optimization process, in the airfoil optimization. Other methods such as Nelder-Mead [7] and Differential Evolution (DE)[27] were performed in the airfoil design as well. A widely used method shall be GA method [29, 42, 45, 1, 31], since GA method has a great deal of merits. Oyama et al.[29] designed an airfoil with GA methods using two-dimensional NS solver. The maximum lift-to-drag ratio was taken as the objective and B-spline function was used to parameterize airfoil. Small surface waves were found on the designed airfoil. Jones [20] combined GA method with XFOIL to optimize an airfoil with the objectives of maximum lift-to-drag ratio and minimum acoustics. Airfoil was parameterized with B-spline function. And high irregular airfoil surface was obtained. Those methods employ either conventional GA method, or modified GA method. The diversity and fitness can't be ensured. Controlled elitist Non-dominated Sorting Genetic Algorithm II (NSGA-II) method proposed by Deb [9] which increases the diversity of population while keeps the elitists in the population is a potential candidate for airfoil optimization method.

The geometry parametric representation of airfoil influences the optimization results as well. From the results of references [29] and [20], airfoils were produced with small surface waves for multi-point optimization. It is analyzed that the application of bad parameterization method and objective function results in those bad results. The geometry representation is necessary before the optimization. Numerous methods [33, 32, 39, 30, 18, 37] including discrete airfoil coordinates method, Bezier or B-Spline control point representation method, free form airfoil representation, polynomial surface representation and cubic spline control point representation, were devised to numerically represent airfoil geometry. Good parametric method can construct the airfoil curve with fewer variables. Selection of a parameterization technique is an important step for airfoil shape design optimization. The parameterization based on the B-Spline has advantages of continuous second-order derivative, fewer design parameters to express various airfoil shapes and intuitive definition of initial design space [29]. However, B-Spline technique produces airfoils with small surface waves for multi-point optimization. Free-form parameterization method can prevent easy manipulation, but it is the lack of intuitive control and the inherent difficulties encountered when trying to generate airfoil-like shapes. Some special parameterization methods such as Hicks-Henne function [18], PARSEC [37] were also developed for certain shape optimization. Kulfan [23, 22] proposed Class function / Shape function Transformation (CST) method including class function and shape function to parameterize geometric shape. This method requires fewer variables to represent airfoil and ensures the smoothness of form.

From the analysis above, it is found that Inverse method and direct method are widely utilized to get the airfoil for a special case directly. An inverse method allows the velocity distribution to be directly controlled rather than anticipated from geometry perturbations, while a direct method allows the design of airfoil with taking into account multi disciplines and multi points. The direct method has more opportunity to get a global optimized solution. Therefore, some study [13] combines the indirect method and direct method in order to eliminate the disadvantages. However, the increase of computational resource and capacity of achieving an optimization method are still under discussed. The representation of airfoil and the process of objective functions have a great impact on the airfoil design since they even determine the efficiency and precision of optimization. The airfoil of nano rotor surfers a large scope of Re so that the airfoil design is a multi-objective optimization. The determination of optimization method coupling with an accurate and efficient aerodynamic solver, an appropriate parameterization method and the process method of objective functions is necessary to obtain a nano rotor airfoil with excellent aerodynamic performance.

In this paper, the airfoil of nano rotor was firstly parameterized with the robust Class func-

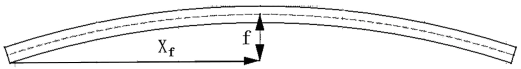

Figure 1: Basic form of plate airfoil.

tion/Shape function Transformation technique (CST). Secondly, the accuracy of aerodynamic solver was verified at ultra-low Reynolds. Then, the objective functions were processed by a method based on the statistical definition of stability. Finally, the airfoil was optimized using controlled elitist Non-dominated Sorting Genetic Algorithm II (NSGA-II) method to ensure the robustness and diversity of the population. And the aerodynamic performance of designed airfoil was computed with two-dimensional (2D) incompressible N-S solver. Comparisons were carried out between the performance of the rotors designed with designed airfoil and ag38 airfoil.

http://www.imavs.org/

2 Geometry Parametric Representation and Aerodynamic Solver

2.1 Geometry Parametric Representation

2.1.1 Basic form of blade airfoil

With the development of MAV, aerodynamic performance of airfoil at low Reynolds turns out to be an interesting field. Enormous experiments and computations have been conducted [43, 40, 16, 21, 5]. Despite the fact that the airfoil presented in those studies can't be used as the airfoil of nano rotor, they can provide this design with some guidelines. A majority of studies show that the thin plate airfoil exhibits better aerodynamic performance than thick NACA airfoil especially when the thickness is lower than 2% of chord. But conclusions vary each other for the other parameters such as camber, location of camber, leading edge angle and roughness etc. Furthermore, the limitation of traditional fabrication method confines the airfoil form. Consequently, the plate airfoil with thickness of 2% is selected as the basic form (Figure 1) to design rotor. However, the camber and location of maximum camber are still remained underdetermined. So optimization method was utilized in the following part to obtain those parameters.

2.1.2 CST Representation Method

In order to optimize airfoil, the airfoil shall be parameterized in advance. Since the plate airfoil was chosen as the basic form, the upper and the lower surfaces of airfoil are able to be represented. The selection of the mathematical representation of an airfoil which is utilized in aerodynamic design optimization has a profound impact on computational time and resources as the selection of the type of optimization algorithm. It also determines whether or not the geometries contained in the design space are smooth or irregular, or even physically realistic or acceptable. It affects the suitability of the selected optimization process. Therefore, the geometric representation technique shall include the characteristics of being capable of producing smooth and realistic shapes, good mathematically efficiency and numerically stability, flexibility, and robustness. After examination of several diverse geometry parametric representation methods, it was found the CST representation methodology illustrates a powerful capability to

represent a wide variety of 2-D and 3-D geometries encompassing a very large design space with a relatively few scalar parameters. CST method is therefore utilized as the geometry parametric representation. For the upper and the lower surfaces, CST functions are

$$Z_U\left(\frac{x}{c}\right) = C_{N_2}^{N_1}\left(\frac{x}{c}\right) \cdot \sum_{r=0}^{n} A_{U,r+1} K_{r,n} \left(\frac{x}{c}\right)^r \left(1-\frac{x}{c}\right)^{n-r} + \frac{x}{c} \cdot \frac{\triangle Z_{UTE}}{c} \tag{1}$$

and

$$Z_L\left(\frac{x}{c}\right) = C_{N_2}^{N_1}\left(\frac{x}{c}\right) \cdot \sum_{r=0}^{n} A_{L,r+1} K_{r,n} \left(\frac{x}{c}\right)^r \left(1-\frac{x}{c}\right)^{n-r} + \frac{x}{c} \cdot \frac{\triangle Z_{LTE}}{c}. \tag{2}$$

where $C_{N_2}^{N_1}$ is the class function, c is the chord length, A_r is the weight of each Bernstein polynomial item, K_r is the Binominal coefficient, and $\triangle Z_{TE}$ is the trailing edge thickness.

Plate airfoil can then be parameterized by the methodology proposed above. To ensure the smoothness of the curve, all the coefficients of Bernstein Polynomial were assumed to be positive. Since the curves of airfoil surfaces are simple, the Bernstein Polynomial is simplified to contain four items. Therefore, there are six parameters to be determined which are $X = (N_1, N_2, A_1, A_2, A_3, A_4)$. To ensue that the airfoil is physically realistic or acceptable, the bounder of array can be constrained in a small zone to reduce the computational time and resource. Since all the parameters are positive, the lower bound and the upper bound were defined to ensure that the equations can cover a wide range of airfoil shape. The results of representation method showed that the airfoil camber varied from 0% to 100% and the location of camber vary from 0% to 100% with the bound defined. And it was found that the value of exponents N_1 and N_2 defines the basic geometry of airfoil, while the value of A_1, A_2, A_3 and A_4 determine the camber and the location of maximum camber. Considering the limitation of computational solver, the leading edge and the trailing edge of airfoil were modified slightly.

2.2 Aerodynamic Solver

The optimization of airfoil requires a good optimization method as well as an accurate solver. XFOIL [12] is an analytical method whose inviscid formulation is a linear-vorticity stream function panel method. A Karman-Tsien compressibility correction with a solution generated from closely coupled viscous and inviscid methods is incorporated. It employs a two-equation, lagged dissipation, integral boundary layer solution strongly interacted with the incompressible potential flow via the surface transpiration model and an envelope e_N transition criterion which allows prediction of separation bubble. While reduced by eliminating the interactive design and plotting features, as well as modified to create a callable function, the analytic capabilities of XFOIL remain unchanged. As a result, lift, drag and moment coefficients can be obtained for airfoils operating through flight conditions in relatively brief periods of time. XFOIL was widely verified for airfoil study at Reynolds number above 15,000, but it was scarcely studied at ultra-low Reynolds. Therefore, the ability of XFOIL to predict the aerodynamic characterization of airfoil at ultra-low Reynolds were validated before the optimization. XFOIL was firstly verified with AG38 airfoil . AG38 airfoil is a thick airfoil with thickness of 7% but a maximum camber of only 2% at 0.355. Youngren et al. [44] studied the aerodynamic characterization of AG38 at low Reynolds number ranging from 15,000 to 60,000 in NASA Langley 23 Boundary Layer Tunnel. Taking account of Reynolds number at which NAV flies, AG38 airfoil was studied with XFOIL at Re of 15,000 at angles of attack ranging from $-4°$ to $8°$. Figure 2 showed that the lift coefficient and drag coefficient vary with angle of attack for both computational results and experimental results. XFOIL predicted the aerodynamic performance well at the whole range of

http://www.imavs.org/

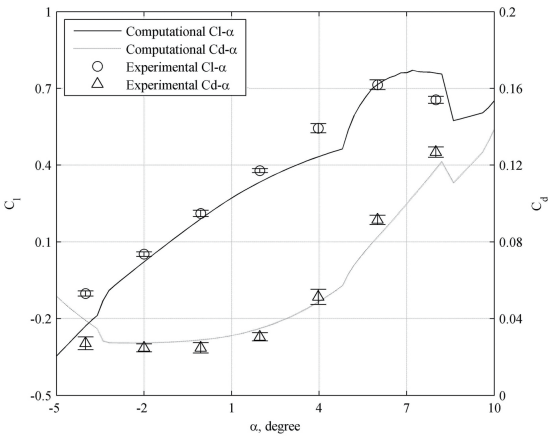

Figure 2: Comparison of computational results with experimental results [44] of AG38 airfoil at Re 15,000.

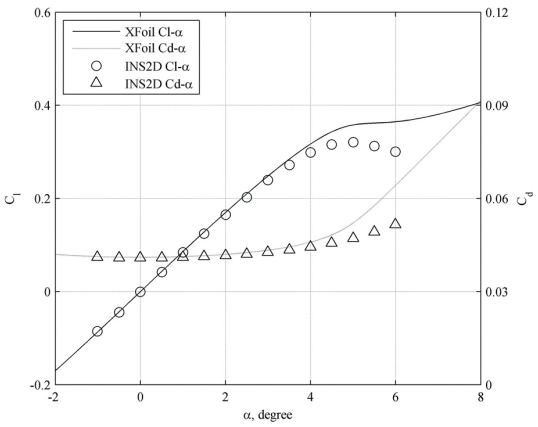

Figure 3: Comparison between computational results for XFOIL and computation results for INS2D [24] of NACA 0006 airfoil at Re 6000.

angle of attack. However, the separation of laminar was predicted earlier since the slope of lift coefficient curve drops slightly at low angles of attack. Accordingly, the value of lift coefficient computed is lower than that from experiments at angles of attack ranging from 2° to 4°, vice verse for drag coefficient. At negative angles of attack lower than −4°, the lift coefficient was under-estimated. One possible reason might be the early estimation of the separation at the upper surface of airfoil. Validation was performed with NACA0006 airfoil at Re of 6,000 as well. Kunz [24] studied the aerodynamic performance of NACA airfoil with INS2D code at low Reynolds from 2,000 to 8,000. INS2D code is two-dimensional incompressible Navier-Stokes solver developed by Rogers in which artificial compressibility method is utilized to deal with incompressible flow. This code was validated by Kunz at low Re. In this validation, NACA0006 airfoil was studied with XFOIL at Re of 6,000 to compare with Kunz's result calculated with INS2D. Figure 3 shows the comparison between the results calculated by XFOIL and Kunz's

http://www.imavs.org/

http://www.imavs.org/

results. The lift coefficient predicted by XFOIL match well with that predicted by INS2D except at high angle of attack. Once stall appears, XFOIL fails to capture the rapid drop of the lift coefficient at angle of attack of 5°. But for the drag coefficient, XFOIL predicts higher value than INS2D after stall.

In summary, XFOIL can predict lift coefficient and drag coefficient well at Re ranging from 6,000 to 15,000 before stall. However, XFOIL predicts the separation earlier. Once attachment appears, lift coefficient is always overestimated.

3 Objective Function Definition Method and Optimization Method

3.1 Objective Function Definition Method

Prior to the procedure of optimization, the objective functions shall be determined. Through the analysis of modern MAVs, it is found that one of the bottlenecks is the power efficiency during the flight, especially with the drop of the flight speed and the decrease of flight vehicle size. Hovering performance is therefore an important parameters to judge the performance of NAV so that it shall be paid more attention during NAV design. To characterize the hovering performance, FM is defined as shown in the following equation

$$FM = \frac{C_T^{3/2}}{2C_P}. \tag{3}$$

According to the blade element theory [25], it was found that FM is a function of $C_l^{3/2}/C_d$ of the airfoil. Therefore, the objective of this optimization is to obtain the maximum value of $C_l^{3/2}/C_d$ of airfoil with the constraint of minimum lift coefficient.

The flow condition suffered by airfoil varies along the blade. Thereafter, the optimization is a multi-objective problem to achieve an airfoil with excellent aerodynamic performance along different stations of rotor blade. Several Res can be treated as the design points since Re varies along the rotor blade. Taking into account the hub of nano rotor, Re range was defined from 6000 to 16,000. Six design points were chosen to optimize the airfoil with equal interval of Re. At each design point, the angle of attack increases from $-2°$ to $10°$ to search for the maximum $C_l^{3/2}/C_d$ with the lift coefficient greater than a specified value $C_{l,spe}$.

A method based on the statistical definition of stability [26] is utilized in the present study to process objectives. The objective to obtain a maximum value of $C_l^{3/2}/C_d$ for this optimization was transformed to obtain a minimum value of $C_d/C_l^{3/2}$ to be able to apply the method. The mean and variance of $C_d/C_l^{3/2}$ with respect to Reynolds are two objective functions defined as,

$$\begin{cases} Minmize f_1(D, Re) & = & E(min(C_d(D, Re)/C_l^{3/2}(D, Re))) \\ Minmize f_2(D, Re) & = & \sigma^2(min(C_d(D, Re)/C_l^{3/2}(D, Re))) \\ subject\ to: & & C_l \geq C_{l,spe} \\ D \in X, & & Re \in (6000, 16,000) \end{cases} \tag{4}$$

3.2 Optimization Method

GA is an optimization algorithm based on Darwin's survival of the fittest evolutionary concept, according to which a biological population evolves over generations to adapt to the environment

http://www.imavs.org/

by selection, recombination and mutation. It was originally described by Holland in 1960s [19]. Since then, GA was well-developed by Holland and his student, namely Goldberg. With the first application of GA to the practice by Goldberg [14], it has been increasingly applied to engineering design and optimization problems. Aerodynamic shape optimization as one of important issues of aerodynamic study profits the development of GA in recent years. The aerodynamic shape optimization of rotor airfoil is a multi-variable and multi-objective problem. GA method can solve this problem by locating a global optimum robustly. For multi-objective optimization, GA finds a local Pareto front for multiple objective functions. The fitness and diversity of population are two criterions to judge the optimal population. The controlled elitist Non-dominated Sorting Genetic Algorithm II (NSGA-II) [9] was therefore applied in the study. NSGA-II applies an elite preserving mechanism and a fast non-dominated sorting procedure assuring the preservation of good solutions found in previous generation and a fast computation. The elimination of tunable parameter increases the independence of the method to user. However, the elite solutions are composed of all solutions belonging to the currently best non-dominated front. A situation which might occur is that not enough new decision variables can be accepted in new population due to the preservation of elitism in previous generation, i.e. the diversity of population is bad. A suboptimal solution set is obtained instead of a global optimal solution. Therefore, the controlled elitist NSGA-II approach was utilized in the design.

3.2.1 NSGA-II

After the determination of objective functions, the process of GA method can be performed. At the beginning, the initial population $G_0 = (D_1^0, D_2^0, \cdots, D_j^0, \cdots, D_N^0)$ is generated randomly according to the bound of the design space. The initial population contained N chromosomes. Each chromosome is composed of six variables. The six variables named genes in the chromosome are capable of representing the geometry of the airfoil. Each gene is generated randomly with their lower and upper bounds.

The fitness functions are defined based on the objective functions as shown below.

$$\begin{cases} F_1 = f_1^{max} - f_1(D, Re) & f_1(D, Re) < f_1^{max} \\ 0 & \text{else.} \end{cases} \tag{5}$$

$$\begin{cases} F_2 = f_2^{max} - f_2(D, Re) & f_2(D, Re) < f_2^{max} \\ 0 & \text{else.} \end{cases} \tag{6}$$

In the function, f_1^{max} and f_2^{max} are the maximum values estimated for objective functions. With initial population, each chromosome is inputted into the XFOIL solver so that the objective functions are calculated and the correspondent fitness function values are achieved as a result. The fitness values for the jth chromosome are represented as $F_{1,j}$ and $F_{2,j}$. After the determination of all fitness values for each chromosome, the population is sorted based on non-domination. The fast sort algorithm proposed by Deb [10] is used in this optimization. Thereafter, all the chromosomes in the population are successively ranked with the no-dominated sort. However, there are usually several individuals in one front. In order to compare these individuals, the crowding distance function is introduced to find the Euclidian distance between each individual. All the individuals are assigned a crowding distance value. The crowing distance is then calculated based on their objectives. Thus, each individual in the population has two properties that are no-domination rank defined as P_{rank} and crowding distance Dis. The non-dominated sort has a computational complexity of $O(MN^2)$where M is the number of genes and N is the number of chromosomes.

http://www.imavs.org/

With the results of sort, a new child population was generated with the binary tournament selection, the recombination and mutation operators. Binary tournament selection has the advantages of high efficiency, translation and scaling invariant, and easy realization of parallel evolutionary algorithms [15]. Therefore, the initial population is processed using binary tournament selection. In order to generate the offspring population of initial population, the simulated binary crossover [3, 8] is utilized to continue process the population obtained from the selection. With the population generated by simulated binary crossover, the polynomial mutation [8] is carried out to generate the final child population defined as GC^0. However, the child population GC^0 isn't the next generation parent population as the other genetic algorithm. The NSGA-II utilizes a combination of parent population G^0 and its child population GC^0 obtained in the initial step to carry out the optimization to ensure elitism as below.

$$R = G^0 \cup GC^0 \tag{7}$$

The fast non-dominated sort is carried out with R as described above. From the first front, the individuals which have high dominance are added to next generation parent population G^1 until the size exceeds the total number of chromosome N. G^1 is the next generation parent population which will be used to produce the next iteration until the convergence.

3.2.2 Controlled Elitist NSGA-II

Despite the fact that the mutation can increase the diversity of population, NSGA-II discards the chromosomes in the pareto front with high rank which deteriorates the diversity of population, especially for the case when the population is mostly comprised of currently best non-dominated solutions. Therefore, a controlled elitist non-dominated sorting GA [9] is utilized here. A geometric distribution is introduced as

$$n_i = N \cdot \frac{(1-r)r^{i-1}}{1-r^K} \tag{8}$$

where n_i , N, r, and K are the maximum number of allowed individuals in the ith pareto front, the number of individuals in the parent population, the reduction rate defined by users and the number of total pareto front, respectively. Because the next parent population has a number of individuals of N, the formula ensures the summary of n_i to be N. If n_i is higher than the number of individuals in ith pareto front, the extra number will be succeeded to the n_{i+1} until the end of sort. In the end the next generation parent population is generated with high fitness and diversity. The procedures above continued until the stopping criteria.

4 Results and Discussion

The nano-rotor blade airfoil optimization was carried out at ultra-low Re using the method above. An initial population of 100 individuals and the number of maximum generation of 200 were set for the controlled elitist NSGA-II method. In order to compute the fitness of each population, XFOIL solver was executed for one hundred times. And in each calculation, the aerodynamic forces of each airfoil shall be computed at several angles of attack. Therefore, the iterations consume huge computational resource. Hereafter, the stop criteria is defined as $f_1(D, Re) < 0.075$ and $f_2(D, Re) < 0.0075$. The stop criteria were satisfied after 120 generations. The pareto front was shown in Figure 4. The results show good diversity along the pareto front which ensures the airfoil parameters are well optimized.The airfoil optimized which

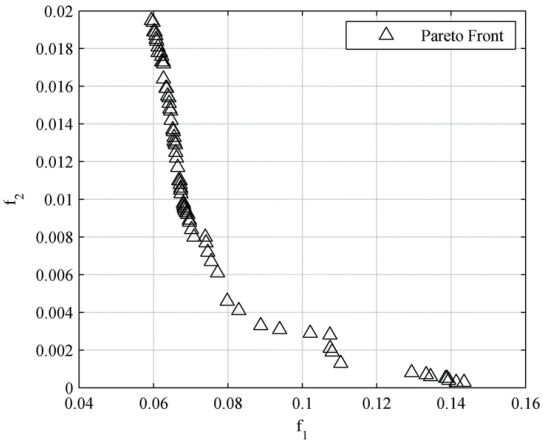

Figure 4: Pareto front of airfoil optimization.

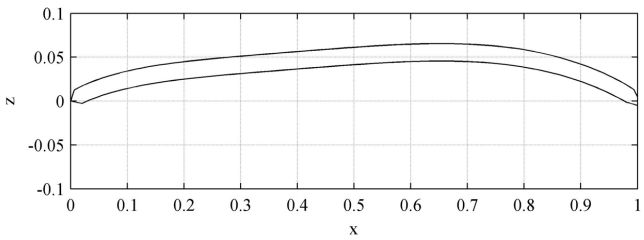

Figure 5: Geometry of airfoil optimized.

http://www.imavs.org/

satisfies the requirement of stop criteria is illustrated in Figure 5. The airfoil has a uniform thickness of 2% with modification at leading edge and trailing edge. The maximum camber is 5.6% at the location of about 2/3. The camber of airfoil is around 5% from 0.4c to 0.8c which is different from the traditional camber line. However, the airfoil optimized approximates to that designed by Kunz for Mesicopter [24].

To verify the accurate aerodynamic performance of airfoil optimized, Computational Fluid Dynamics (CFD) method was used to simulate the flow field of airfoil. For low-Mach and low-Re flow, conventional NS equations might fail to converge to a correct solution. Therefore, 2D incompressible Navier-Stokes (INS) solver with artificial compressibility was used to compute the aerodynamic performance of airfoil optimized at ultra-low Re. Because of the special flight condition of nano rotor, the airfoil suffers flows at a wide Re range. The airfoil is simulated at typical Reynolds numbers from 6,000 to 16,000 with an interval of 2,000. At each Re, the angle of attack varies with an increment of 2°. The grid of the airfoil was shown in Figure 6. The size of mesh is 16151 points in the streamwise and the normal direction, respectively. At the leading edge and trailing edge, more grid points were distributed to capture the flow characteristics. The width of the first layer of grid is 1.0×10^{-4}.

The pressure coefficient contours at angle of attack of 4° were presented in Figure 8. According to the contours, high pressure was generated on the lower surface of airfoil while lower pressure was generated on the upper surface. And complicate vortices were found at the trailing edge of airfoil, especially at Re 16,000. So, unsteady aerodynamic phenomena appear for airfoil

http://www.imavs.org/

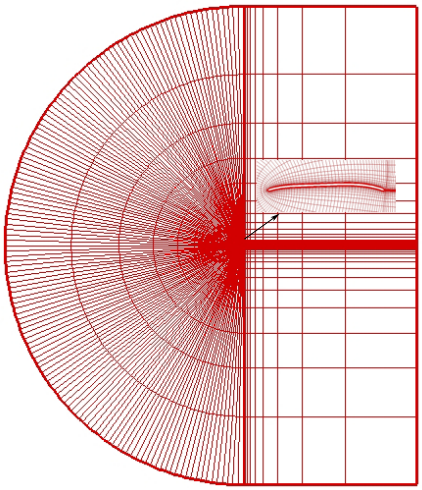

Figure 6: Grid of airfoil optimized.

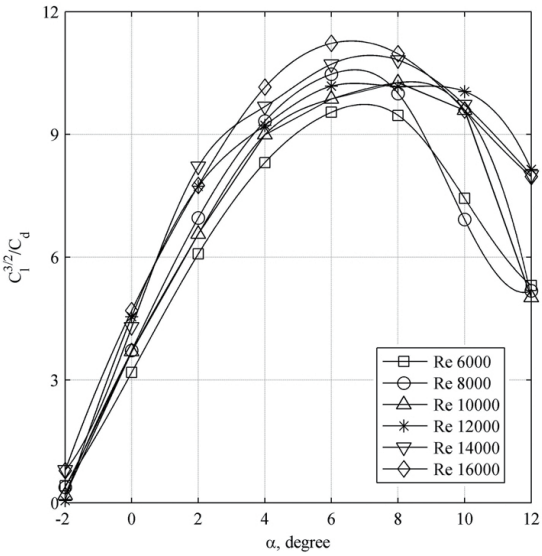

Figure 7: $C_l^{3/2}/C_d$ varying with angle of attack at different Res for optimized airfoil.

optimized at low Re. Figure 7 illustrates $C_l^{3/2}/C_d$ calculated by INS solver varies with angle of attack at Re ranging from 6,000 to 16,000 for optimized airfoil. Results show that $C_l^{3/2}/C_d$ increases with the Reynolds number in general but it varies from angle of attack as well. Generally, reaches a maximum value at angle of attack of 6°. The maximum is from 9.5 to 11.2 which are lower than that predicted by the XFOIL. However, they still reach a relatively high value at ultra-low Re when comparing with other airfoils. The maximum $C_l^{3/2}/C_d$ of airfoil AG38 is only 7.8 at Re 15,000 and 9.5 at Re 20,000 [44]. The maximum $C_l^{3/2}/C_d$ of airfoil NACA0006 at Re 6,000 is about 3.9, whereas it is about 9.5 for optimized airfoil at the same

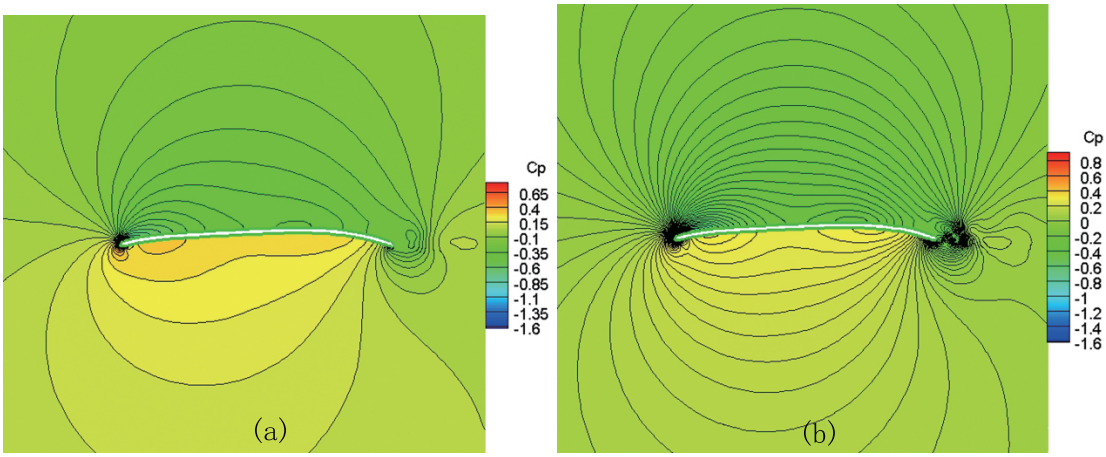

Figure 8: Pressure coefficient contours of airfoil optimized: (a)Reynolds number 8,000; (b)Rynolds number 16,000.

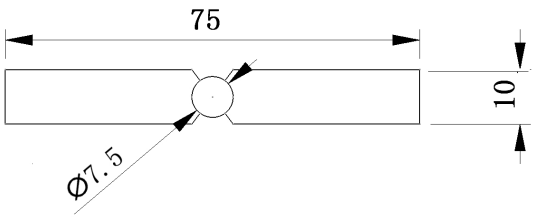

Figure 9: Simple rotor(unit:mm).

Re [24]. Lift coefficient increases while drag coefficient decreases with the increase Re, so better aerodynamic performance can be obtained at higher Re. But the irregular phenomena appear at certain Re or angle of attack due to the unsteady characteristic of ultra-low Re flow.

Simple rotors with diameter of 75mm and uniform blade chord length of 10mm were generated with optimized airfoil and ag38 airfoil as shown in Figure 9, respectively. The performance of both rotors were compared so as to verify the priority of optimized airfoil. Calculations were performed with RPM of 6500 for both rotors while pitch angle varied from 0 to 12 degree using potential goldstein formulation method. Figure 10 showed Figure of Merit(FM) varying with the ratio of thrust coefficient to solidity for both rotors. It was found that the thrust of coefficient reached a higher value for optimized airfoil. The value of FM of rotor designed with ag38 airfoil, named as rotor 2, was higher than that of rotor designed with optimized airfoil, named as rotor 2, when the thrust coefficient remained as a small value. However, FM of rotor 2 increased sharply with thrust coefficient and a maximum value of about 0.8 was obtained in comparison with only 0.5 for rotor 1. Rotor 2 exhibited a better performance than rotor 1 at high thrust coefficient.

http://www.imavs.org/

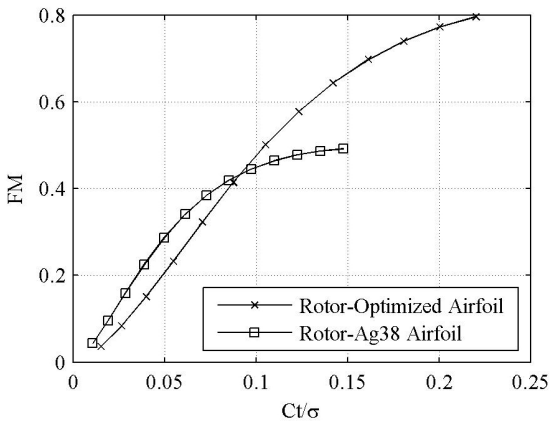

Figure 10: Figure of merit varying with ct/σ.

http://www.imavs.org/

5 Conclusion

The performance of airfoil has a direct impact on aerodynamic performance of rotor. In this paper, the optimization of airfoil for nano rotor was carried out at ultra-low Re. In order to optimize the airfoil, parameterization method which has an impact on the efficiency and precision of airfoil optimization was determined. A CST representation algorithm was selected to parameterize the airfoil after a survey of several different representation methods due to its simplicity and robustness. CST can represent current plate airfoil with a few variables and guarantee the continuity and smoothness of the airfoil form. The plate airfoil was represented with six design variables whose bounds were determined based on CST to simplify the optimization. Successively, the flow solver was verified. Because of the ultra-low Re suffered by nano rotor and the requirement of numerous computational resources, the flow solver shall have the capacities of solving the ultra-low Re flow accurately and efficiently. In this optimization, XFOIL, which is widely verified at low Re, was used. At several low Res, XFOIL solver was verified with multiple airfoils and the computational results were compared with those from experiments and CFD. It is evident that XFOIL can calculate the aerodynamic performance of different types of airfoils accurately before the stall, not only for lift, but also for drag. It is concluded that it is applicable to used XFOIL as the solver of optimization. Subsequently, the airfoil was optimized. Controlled elitist NSGA-II optimization method was employed to design nano rotor airfoil combing with the CST parameterization method and the statistical definition of stability objective-function-process method. It is innovatively proposed that the objective of this optimization is to obtain the maximum value of $C_l^{3/2}/C_d$ of airfoil instead of lift-to-drag ratio with the constraint of minimum lift coefficient. Several Res were chosen as the design points to obtain an excellent airfoil along the blade. The mean and the standard deviation of the values of objectives at the design points were taken as the objective functions based on the method of the statistical definition of stability. Controlled elitist NSGA-II method was then utilized to design nano rotor airfoil. A plate airfoil with maximum thickness of 2% and maximum camber of 5.6% at 2/3 was achieved. The optimization airfoil exhibits good aerodynamic performance at ultra-low Re. When comparing rotors' performance designed with optimized airfoil and ag38 airfoil, it was found that rotor designed with optimized airfoil can achieve a high FM and exhibited a better performance at high thrust coefficient, which proved

that the optimization methods are suitable for rotor airfoil design.

In conclusion, controlled elitist NSGA-II method combining with CST parameterization method and the statistical definition of stability objective-function-process method was successfully employed on airfoil design. A plate airfoil was designed and exhibited excellent aerodynamic performance.

6 Future Work

During the design of nano coaxial rotor airfoil, the solver of XFOIL was used. XFOIL has a certain precision to simulate airfoil at ultra-low Re, but it fails to predict the aerodynamic performance of airfoil after stall. Therefore, other solver with higher precision and efficiency can be employed. GA method has the advantages of robustness and independence from initial solutions. However, it requires a large amount of computational recourses. Therefore, GA method can be used to obtain a solution as the initial solution of the other efficient optimization method.

7 Acknowledgments

The authors would like to thank the support of Natural Science Foundation of Shaanxi Province(Grant No. 2012JQ1018) and the Fundamental Research Funds for the Central Universities. They would also like to thank the laboratory of DAEP of ISAE.

References

[1] V. Ahuja and A. Hosangadi. Design optimization of complex flowfields using evolutionary algorithms and hybrid unstructured cfd. In *17th AIAA Computational Fluid Dynamics Conference*, pages 2005–4984. AIAA E-library, June 2005.

[2] N. M. Alexandron, E. J. Nielsen, R. M. Lewis, and et al. First-order model management with variable-fidelity physics applied to multi-element airfoil optimization. In *8th AIAA/USAF/-NASA/ISSMO Symposium on Multidisciplinary Analysis and optimization*, pages 2000–4886. AIAA E-library, June 2000.

[3] H. G. Beyer and K. Deb. On self-adaptive features in real-parameter evolutionary algorithm. *IEEE Transactions on Evolutionary Computation*, 5(3):250–270, 2001.

[4] F. Bohorquez. *Rotor hover performance and system design of an efficient coaxial rotarywing Micro Air Vehicle*. PhD thesis, University of Maryland,US, 2007.

[5] F. Bohorquez, F. Rankins, J. D. Daeder, and et al. Hovering performance of rotor blades at low reynolds numbers for rotary wing micro air vehicles-an experimental and cfd study. In *21st AIAA Applied Aerodyanmics Conference*, pages 2003–3930. AIAA E-library, June 2003.

[6] G. W. Burgree and O. Baysal. Aerodynamic shape optimization using preconditioned conjugate gradient methods. *AIAA Journal*, 32(11):2145–2152, 1994.

[7] M. Darbandi, A. Setayeshgar, and S. Vakili. Modification of standard k-epsilon turbulence model for multi-element airfoil application using optimization technique. In *AIAA 24th Applied Aerodynamics Conference*, pages 2006–2829. AIAA E-library, June 2006.

[8] K. Deb and R. B. Agarwal. Simulated binary crossover for continuous search space. *Complex System*, 9(1):115–148, 1995.

[9] K. Deb and T. Goel. Controlled elitist non-dominated sorting genetic algorithms for better convergence. Technical report, Springer-Verlag, Heidelberg, 2001.

http://www.imavs.org/

http://www.imavs.org/

[10] K. Deb, A. Pratap, S. Agarwal, and et al. A fast elitist multiobjective genetic algorithm: Nsga-ii. *IEEE Transaction on Evolutionary Computation*, 6(2):182–197, 2002.

[11] M. Drela. Pros and cons of airfoil optimization. In *Frontiers of Computational Fluid Dynamics*, page 1998. World Scientific, June 1998.

[12] M. Drela and H. Youngren. Xfoil 6.94 user guide. [online], 2001. `http://www.mit.edu`.

[13] B. A. Gardner and M. S. Selig. Airfoil design using genetic algorithm and an inverse method. In *41st Aerospace Sciences Meeting and Exhibit*, pages 2003–43. AIAA E-library, June 2003.

[14] D. E. Goldberg. Genetic algorithms in search, optimization and machine learning. Master's thesis, Addison Wesley Reading, USA, 1989.

[15] D. E. Goldberg and K. Deb. A comparative analysis of selection schemes used in genetic algorithms. In *In Foundations of Genetic Algorithms*, page 1998. IEEE Press, June 2001.

[16] A. Gopalarathnam, B. A. Broughton, B. D. McGranahan, and et al. Design of low reynolds number airfoils with trips. In *19th AIAA Applied Aerodynamics Conference*, pages 2001–2463. AIAA E-library, June 2001.

[17] R. He and S. Sato. Design of a single-motor nano aerial vehicle with a gearless torque-canceling mechanism. In *46th AIAA Aerospace Sciences Meeting and Exhibit*, pages 2008–1417. AIAA E-library, June 2008.

[18] R. M. Hicks and P. A. Henne. Wing design by numerical optimization. *Journal of Aircraft*, 15(1):407–412, 1978.

[19] J. H. Holland. Adaptation in natural and artificial system. Master's thesis, Stanford University, USA, 1992.

[20] B. R. Jones, W. A. Crossley, and A. S.Lyrintzis. Aerodynamic and aeroacoustic optimization of airfoils via a parallel genetic algorithm. In *7th AIAA/USF/NASA/ISSMO Symposium on Multidisciplinary Analysis and Optimization*, pages 1998–4811. AIAA E-library, June 1998.

[21] I. Kroo and P. Kunz. The mesicopter: aminiature rotorcraft concept. Technical report, Stanford Univeristy, Palo Alto, 2000.

[22] B. M. Kulfan. A universal parametric geometry representation method-cst. In *45th AIAA Aerospace Sciences Meeting and Exhibit*, pages 2007–62. AIAA E-library, June 2007.

[23] B. M. Kulfan and J. E. Bussoletti. Fundamental parametric geometry representations for aircraft component shapes. In *11th AIAA/ISSMO Multidisciplinary Analysis and Optimization Conference*, pages 2006–6948. AIAA E-library, June 2006.

[24] P. J. Kunz. *Aerodynamics and design for ultra-low Reynolds number flight.* PhD thesis, Stanford University, USA, 2003.

[25] J. G. Leishman. *Principles of helicopter aerodynamics.* CambridgeUniv. Press, New York, 2005.

[26] W. Li and S. Padula. Performance trades study for robust airfoil shape optimization. In *21st Applied Aerodynamics Conference*, pages 2003–3790. AIAA E-library, June 2003.

[27] N. K. Madavan. On improving efficiency of differential evolution for aerodynamic shape optimization applications. In *10th AIAA/SSMO Multidisciplinary Analysis and Optimization Conference*, pages 2004–4622. AIAA E-library, June 2004.

[28] M. Nemec and M. J. Aftosmis. Aerodynamic shape optimization using a cartesian adjoint method and cad geometry. In *24th AIAA Applied Aerodynamics Conference*, pages 2001–3456. AIAA E-library, June 2006.

[29] A. Oyama and K. Fujii. Aerodynamic design exploration of flapping wing viewpoint of shape and kinematics. In *45th AIAA Aerospace Science meeting and Exhibit*, pages 2007–481. AIAA E-library, June 2007.

[30] S. Padula and W. Li. Options for robust airfoil optimization under uncertainty. In *9th AIAA Multidisciplinary Analysis and Optimization Symposium*, pages 2002–5602. AIAA E-library, June 2002.

[31] S. Peigin and B. Epstein. 3d optimization of aerodynamic wings based on accurate cfd computa-

tions. In *43rd AIAA Aerospace Sciences Meeting and Exhibit*, pages 2005–454. AIAA E-library, June 2005.

[32] G. M. Robinson and A. J. Keane. Concise orthogonal representation of supercritical airfoils. *Journal of Aircraft*, 38(3):580–583, 2001.

[33] J. A. Samareh. Survey of shape parameterization techniques for high-fidelity multidisciplinary shape optimization. *AIAA Journal*, 39(5):877–884, 2001.

[34] M. Secanell and A. Suleman. Sequential optimization algorithms for aerodynamic shape optimization. In *10th AIAA/ISSMO Multidisciplinary Analysis and Optimization Conference*, pages 2004–4631. AIAA E-library, June 2004.

[35] M. S. Selig and M. D. Maughmer. Generalized multipoint inverse airfoil design. *AIAA Journal*, 30(11):2618–2625, 1992.

[36] M. S. Selig and M. D. Maughmer. A multi-point inverse airfoil design method based on conformal mapping. *AIAA Journal*, 30(5):1162–1170, 1992.

[37] H. Sobieczky. Parametric airfoils and wings. *Notes on Numerical Fluid Mechanic*, 68(1):71–88, 1998.

[38] B. I. Soemarwoto. Airfoil optimization using the navier-stokes equations by means of the variational method. In *16th Applied Aerodynamics Conference*, pages 1998–2401. AIAA E-library, June 1998.

[39] W. Song and A. J. Keane. A study of shape parameterisation airfoil optimization. In *10th AIAA/ISSMO Multidisciplinary Analysis and Optimization Conference*, pages 2004–4482. AIAA E-library, June 2004.

[40] S. Sunada, T. Yasuda, K. Yasuda, and et al. Comparison of wing characteristics at an ultralow reynolds number. *Journal of Aircraft*, 39(2):331–338, 2002.

[41] C. H. Sung and J. H. Kwon. Design optimization using the navier-stokes and adjoint equations. In *39th AIAA Aerospace Sciences Meeting and Exhibit*, pages 2001–266. AIAA E-library, June 2001.

[42] S. Takahashi, W. Yamazaki, and K. Nakahashi. Aerodynamic design exploration of flapping wing viewpoint of shape and kinematics. In *45th AIAA Aerospace Science meeting and Exhibit*, pages 2007–481. AIAA E-library, June 2007.

[43] Noriaki Tsuzuki, Shunichi Sato, and Takashi Abe. Design guidelines of rotary wings in hover for insect-scale micro air vehicle applications. *Journal of Aircraft*, 44(1):252–263, 2002.

[44] H. Youngren, C. Kroninger, M. Chang, and et al. Low reynolds number testing of the ag38 airfoil for the samarai nano air vehicle. In *46th AIAA Aerospace Sciences Meeting and Exhibit*, pages 2008–417. AIAA E-library, June 2008.

[45] Z .Q. Zhu, X. L. Wang, H. Y. Fu, and et al. Aerodynamic optimization design of airfoil and wing. In *10th AIAA/SSMO Multidisciplinary Analysis and Optimization Conference*, pages 2004–4367. AIAA E-library, June 2004.

http://www.imavs.org/